Proceedings of *RAGtime 14–16, 18–22 Sept./15–18 July/11–19 Oct., '12/'13/'14, Opava, Prague, Czech Republic*
Z. Stuchlík, G. Török and T. Pecháček, editors, Silesian University in Opava, 2014, pp. 193–204

Geometrically thin accretion disk around Maclaurin spheroids

Bhupendra Mishra[1] and Bhargav Vaidya[2]

[1]Nicolaus Copernicus Astronomical Center, Bartycka 18, 00-716 Warsaw, Poland
[2]Dipartimento di Fisica 'Amedeo Avogadro' Università degli Studi di Torino
Via Pietro Giuria 1, 10125 Torino, Italy

ABSTRACT
We studied a semi-analytic and numerical model of geometrically thin disk around Maclaurin spheroid. We are mainly interested in the inner region of the so called alpha-disk, alpha being the viscosity parameter. We found minor changes in the emitted spectra from the disk for a change in eccentricity of Maclaurin spheroid. We also found that change in eccentricity of Maclaurin spheroid changes various disk parameters like disk thickness, surface density and central temperature. Numerical work has been carried out to see the viscous time evolution of the non-stationary accretion disk around Maclaurin spheroid. In numerical model we showed that if the eccentricity of the Maclaurin spheroid is high the matter will diffuse slowly during the disk evolution.

Keywords: accretion – accretion disk – hydrodynamics – stars: neutron

1 INTRODUCTION

Geometrically thin accretion disks have been studied intensively in last few decades using some very robust models. The best known analytic models for describing the accretion disk were proposed by Shakura and Sunyaev (1973), Novikov and Thorne (1973) and Lynden-Bell and Pringle (1974). Shakura and Sunyaev (1973) considered Newtonian potential around spherically symmetric body (black hole). To investigate relativistic effects due to strong gravity in the accretion process a different choice of potential or metric is required. Novikov and Thorne (1973) considered thin accretion disk around rotating black holes using Kerr space-time. Novikov and Thorne (1973) solutions are extension of Newtonian results by Shakura and Sunyaev (1973) to relativistic regime.

Using relativistic approach Kovács et al. (2009) solved the non-stationary thin accretion disk around quark stars. Gondek-Rosińska et al. (2014) calculated the effect of eccentricity of quark-star on the orbital frequencies to investigate the quasi periodic oscillations (QPOs). Recently Khanna et al. (2014) computed trapped horizontal modes in accretion disk around Maclaurin spheroids. Bisnovatyi-Kogan (1993) studied the correlation between mass accretion rate and eccentricity of the rapidly rotating star. In the same trend we performed a semi-analytic and numerical study of viscous (constant 'alpha') accretion disk around

978-80-7510-127-3

a Maclaurin spheroid. We used Maclaurin spheroid potential for a constant density and mass central object. This model describes that how the Maclaurin spheroid potential will affect the dynamics of accreting matter. We are focused only close to Maclaurin spheroid to have the effects of multipoles in our calculations. As a first attempt we assumed constant α viscosity prescription to proceed with analytic and numerical work.

In Maclaurin spheroid potential there occurs an innermost stable circular orbit (ISCO) even in Newtonian dynamics (Amsterdamski et al., 2002; Kluźniak and Rosińska, 2013). We chose a constant density and mass Maclaurin spheroid and assumed that it is rotating rapidly. Rapid rotation of Maclaurin spheroid can change its eccentricity and so semi-major axis. In Kluźniak and Rosińska (2013), it has been shown that if the eccentricity is less than a critical value of $e_c = 0.8345$, the ISCO will lie on the equator of the accreting source but if it is higher than this value it will be detached from the surface of the star. Keeping this change in mind we investigated the cases where eccentricity is less than critical limit. We see a change in inner radius of the accretion disk with change in eccentricity because the semi-major axis of the accreting Maclaurin spheroid is changing. We also simulated the non-stationary accretion disk around Maclaurin spheroid by solving the diffusion equation for the accreting matter. We again assumed the Maclaurin spheroid potential to proceed with the study of non-stationary disk.

The article is organized in the following manner. In Section 2 we describe physical model of accretion disk which covers steady thin disk and also numerical study of the time evolution of the accretion disk. Section 3 is devoted for describing all the results we obtained analytically and numerically. In Section 4 we discuss all the results described in Section 3 and we conclude in Section A with future applications of our accretion disk model around Maclaurin spheroids. A more general and detailed description of this article can be found in Mishra and Vaidya (2015).

2 PHYSICAL MODEL

2.1 Maclaurin Spheroid

We considered Maclaurin spheroid potential and followed Shakura and Sunyaev (1973) alpha disk model. We assumed ideal gas equation of state for computing the gas pressure. The semi-major axis a of the Maclaurin spheroid changes with eccentricity because we assume constant density and mass Maclaurin spheroid. We also assumed that the disk terminates at the surface of the Maclaurin spheroid. This assumption causes a change in semi-major axis and so inner radius of the accretion disk due to change in eccentricity. The semi-major axis of the Maclaurin spheroid is defined as a function of its radius for $e = 0.0$,

$$a = R_0/\left(1 - e^2\right)^{1/6}, \tag{1}$$

where a is the semi-major axis of the Maclaurin spheroid and R_0 is the semi-major axis of Maclaurin spheroid for eccentricity, $e = 0.0$. The maximum value of eccentricity we chose in this paper is $e = 0.8345$. There is a reason behind choosing this limit, in case of potential for Maclaurin spheroid the radial epicyclic frequency has maximum at $r = \sqrt{2}ae$ for

spheroid eccentricities $e > 1/\sqrt{2}$ but it vanishes for $e_c = 0.83458318$ at the equator of the star (Kluźniak and Rosińska, 2013). With further increase in the eccentricity $e > e_c$, the innermost stable circular orbit (ISCO) will be separated from the equator of star and it will be at $r_{ms} = 1.198203\,ae$ (Kluźniak and Rosińska, 2013). Following this assumption we always kept the inner radius at no-torque boundary (the radius at which the viscosity is zero) which coincides with the variable semi-major axis of Maclaurin spheroid. One can increase the eccentricity further to investigate the accretion disk for which the inner radius does not lie at the surface of Maclaurin spheroid but in this paper we shall not discuss it. The angular velocity (orbital frequency) in case of Maclaurin spheroid potential is given by

$$\Omega^2\,(e, r) = 2\pi G\rho_*\left(1 - e^2\right)^{1/2} e^{-3}\left[\gamma_r - \cos\gamma_r \sin\gamma_r\right]\,, \tag{2}$$

where $\gamma_r = \arcsin(ae/r)$, a is the semi-major axis of Maclaurin spheroid and ρ_* is constant density of the Maclaurin spheroid (Kluźniak and Rosińska, 2013). Now we have angular velocity of the matter for Maclaurin spheroid potential, next goal is to follow Shakura and Sunyaev (1973) alpha disk model and do the calculations for angular velocity calculated from Eq. (2). This analytic approach gave us various disk parameters like, half-thickness, surface density, temperature and radial velocity in the inner, middle and outer region of the accretion disk.

2.2 Steady thin accretion disk

We considered a thin accretion disk (height of disk is much smaller than its radial width) around Maclaurin spheroid. Calculations are done in cylindrical coordinate system (r, ϕ, z), assuming azimuthal symmetry. The goal of this model is to study the steady-state disk and see the behaviour of disk parameters and emitted spectra of the stationary accretion disk. To proceed the calculations for steady-state disk we used Eqs. (2) and (3) to analytically calculate disk parameters in inner region of the accretion disk. The angular momentum equation in terms of angular velocity of accreting matter is given by

$$-v_r\,\Sigma\frac{\mathrm{d}\Omega r^2}{\mathrm{d}r} = \frac{1}{r}\frac{\mathrm{d}}{\mathrm{d}r}W_{r\phi}r^2\,, \tag{3}$$

where v_r is the radial velocity, $W_{r\phi}$ is the stress between adjacent layers (Shakura and Sunyaev, 1973), which is assumed to be a function of sound speed v_s and surface density Σ.

$$\Sigma = 2\int_0^{z_0}\rho\,\mathrm{d}z\,, \tag{4}$$

$$W_{r\phi} = -\alpha\,\Sigma\,v_s^2\,, \tag{5}$$

where α is constant viscosity coefficient. In stationary disk model $\dot{M} = -2\pi\,\Sigma\,v_r r = \text{const}$ and $v_r < 0$. Integrating Eq. (3) gives

$$\dot{M}\,\Omega r^2 = -2\pi\,W_{r\phi}r^2 + \mathrm{C}\,, \tag{6}$$

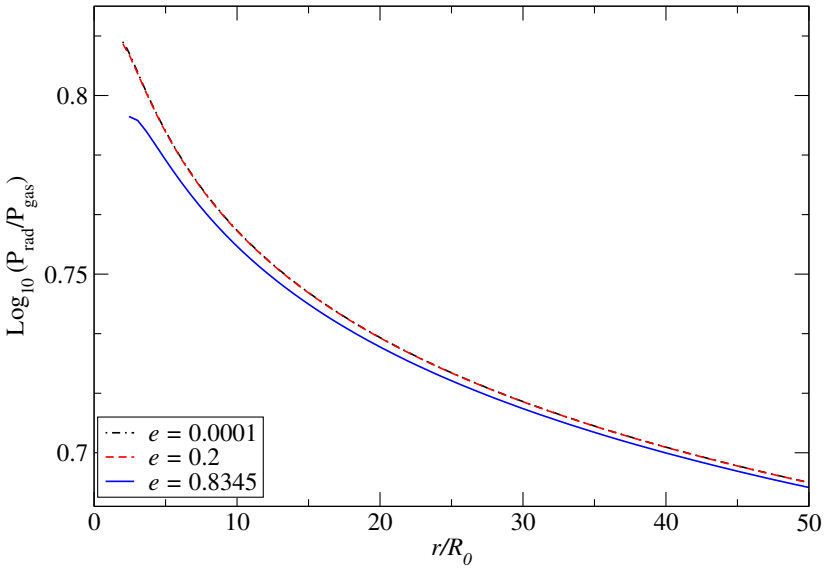

Figure 1. Plot shows the region of interest (*inner region*). The vertical axis shows the ratio of radiation pressure $P_{\rm rad}$ to gas pressure $P_{\rm gas}$. The horizontal axis corresponds to radial distance from the center of the star. Three different eccentricities $e = 10^{-4}$ (*black dotted-dashed curve*), $e = 0.2$ (*red dashed curve*) and $e = 0.8345$ (*solid blue curve*) have been shown in the plot.

where C is constant which we calculated by using no-torque boundary condition (Shakura and Sunyaev, 1973). Finally we get the equation to calculate disk parameters in all three regions of the accretion disk.

$$\dot{M}\left(\Omega r^2 - \Omega(a)a^2\right) = 2\pi\alpha\Sigma v_{\rm s}^2 r^2\,. \tag{7}$$

Now the energy flux radiated from the surface unit as function of $\Omega(e, r)$ is given by

$$Q = -\frac{\dot{M}\left(\Omega r^2 - \Omega(a)a^2\right)}{4\pi r}\frac{{\rm d}\Omega}{{\rm d}r}\,. \tag{8}$$

using Eq. (7) and Eq. (8) together with assumption of radiation pressure dominated region we calculated disk thickness, surface density, temperature and radial velocity in the inner (radiation pressure dominated) region of the accretion disk.

2.2.1 Radiation pressure dominated region

In the same fashion like Shakura and Sunyaev (1973), we formulated three different regions in the accretion disk, the inner one is radiation pressure dominated where in the interaction of matter and radiation electron scattering on free electrons has dominating contribution. Figure 1 verifies our claim that we are studying the inner radiation pressure dominated region. We substituted $\Omega(e, r)$ in Eq. (7) and Eq. (8) from Eq. (2) to calculate the disk

parameters like disk half thickness $z_0(r)$, surface density $\Sigma(r)$, central temperature $T(r)$ and radial velocity $v_{\rm r}(r)$ of the matter. We expressed the analytic expression in terms of defined parameters γ_r, γ_a, p_r, p_a and k_1 to abbreviate the complicated expressions.

$$z_0(r) = \sigma \dot{M} \sin^2 \gamma_r \tan \gamma_r \, (8\pi \, p_r c)^{-1} \left(1 - \left(\frac{p_a}{p_r}\right)^{1/2} \left(\frac{a}{r}\right)^2\right), \tag{9}$$

$$\Sigma(r) = 32\pi c^2 p_r^{3/2} \tan^2 \gamma_r \left(\alpha\sigma^2 k_1^{1/2} \dot{M}\right)^{-1} \left(1 - \left(\frac{p_a}{p_r}\right)^{1/2} \left(\frac{a}{r}\right)^2\right)^{-1}, \tag{10}$$

$$\varepsilon(r) = 6c p_r^{3/2} k_1^{1/2} \left(\alpha\sigma \sin^2 \gamma_r \tan \gamma_r\right)^{-1}, \tag{11}$$

$$T(r) = \left(\varepsilon(r)/b\right)^{1/4}, \tag{12}$$

$$\tau(r) = \sqrt{0.11\sigma_{\rm T} T(r)^{-7/2} n(r)}\, \Sigma(r), \tag{13}$$

$$n(r) = \Sigma(r)/2mpz_0(r), \tag{14}$$

$$v_r(r) = -\dot{M}/2\pi \, \Sigma(r) r, \tag{15}$$

where,

$$k_1 = 2\pi G\rho_* \left(1 - e^2\right)^{1/2} e^{-3}, \tag{16}$$

$$\gamma_r = \arcsin\left(ae/r\right), \tag{17}$$

$$\gamma_a = \arcsin(e), \tag{18}$$

$$p_r = (\gamma_r - \sin\gamma_r \cos\gamma_r), \tag{19}$$

$$p_a = (\gamma_a - \sin\gamma_a \cos\gamma_a). \tag{20}$$

$\dot{M}$ is mass accretion rate, σ is opacity, $b = 3\sigma_{\rm b}/c$ where $\sigma_{\rm b}$ is Stefan Boltzmann constant, $\sigma_{\rm T}$ is Thomson cross-section of electron, $z_0(r)$ is half-thickness of the disk, $\Sigma(r)$ is the radial distribution of surface density, $\varepsilon(r)$ is radial distribution of energy density, $T(r)$ is radial distribution of the central temperature, $\tau(r)$ is optical thickness, $n(r)$ is the number density and $v_{\rm r}(r)$ is the radial velocity of the matter in the steady thin accretion disk.

2.3 Non-stationary accretion disk

In this model we numerically solved the time evolution of the geometrically thin accretion disk around Maclaurin spheroid. The viscous friction causes a transport of angular momentum outwards and matter accretion on to the Maclaurin spheroid. We numerically integrated the diffusion equation Eq. (21) with constant viscosity ν as a first approximation. We used Crank–Nicolson method which is described in Birnstiel et al. (2010) to solve the diffusion-advection equation in code units. The equation we present here can be used to solve the time evolution of accretion disk around different potentials or orbital frequency.

$$\frac{\partial \Sigma}{\partial t} = -\frac{1}{r}\frac{\partial}{\partial r}\left[\frac{1}{2\pi\left(r^2\Omega\right)'}\frac{\partial G}{\partial r}\right], \tag{21}$$

$$v_{\rm r} = \frac{1}{2\pi r \Sigma (r^2 \Omega)'} \frac{\partial G}{\partial r} \,, \tag{22}$$

where,

$$G(r,t) = 2\pi r \nu \Sigma r^2 \Omega' \tag{23}$$

is the torque exerted by two adjacent rings to each other in the accreting matter. Now if we choose the Keplerian angular velocity the above equations reduce to diffusion equation used for study of accretion disk evolution by various models based on Newtonian potential of a spherically symmetric body (Lynden-Bell and Pringle, 1974).

$$\frac{\partial \Sigma}{\partial t} = \frac{3}{r} \frac{\partial}{\partial r} \left[r^{1/2} \frac{\partial}{\partial r} \left(\nu \Sigma r^{1/2} \right) \right] , \tag{24}$$

$$v_r = -\frac{3}{\Sigma r^{1/2}} \frac{\partial}{\partial r} \left(\nu \Sigma r^{1/2} \right) , \tag{25}$$

where Σ is the surface density, ν is kinematic viscosity and $v_{\rm r}$ is the radial velocity. Now using Eqs. (2), (21) and (22) we shall compute the time evolution of the accretion disk for different eccentricities e of the Maclaurin spheroid. Depending on eccentricity e, matter can be diffused either rapidly or slowly.

3 RESULTS

3.1 Steady state disk

In our calculations the radius of Maclaurin spheroid for $e = 0.0$ is $R_0 = 10^6$ cm. This radius will also work for our scaling of radial distance. The constant density of Maclaurin spheroid is $\rho_* = 10^{15}\,{\rm g\cdot cm^{-3}}$. In this article we kept accretion rate fixed at $\dot{M} = 10^{17}\,{\rm g\cdot s^{-1}}$ and changed the eccentricity e of the central object to see the effect on the disk thickness, surface density, temperature and radial velocity of accreting matter in the inner region of accretion disk. We chose three values of eccentricity which are $e = 10^{-4}$, $e = 0.8345$ with an intermediate value of $e = 0.2$. Figure 2 presents the radial variation of the half-thickness $z_0(r)$, surface density $\Sigma(r)$, central temperature $T(r)$ and radial velocity $v_{\rm r}(r)$. In this figure the inner grid point of the plot for all the parameters is $2R_0$ to avoid singularities at the inner boundary of the disk. We see from upper left panel a difference in the half thickness of the accretion disk for different eccentricities $e = 10^{-4}$ (black dashed-dotted curve), $e = 0.2$ (red dashed curve) and $e = 0.8345$ (solid blue curve). Higher eccentricity e of the star corresponds to lower disk thickness at a particular radial distance from the center of Maclaurin spheroid. The upper right panel shows the logarithmic variation of the surface density distribution in the inner region of the accretion disk. We see that for higher eccentricities the surface density is higher than for the lower eccentricities. The surface density $\Sigma(r)$ also increases with radial distance in the inner region of the accretion disk. The lower left panel shows the radial variation of central temperature $T(r)$ in the accretion disk. The lower right panel shows the radial velocity profile $v_{\rm r}(r)$ in the accretion disk. We see a very small difference in radial velocity for different eccentricities e.

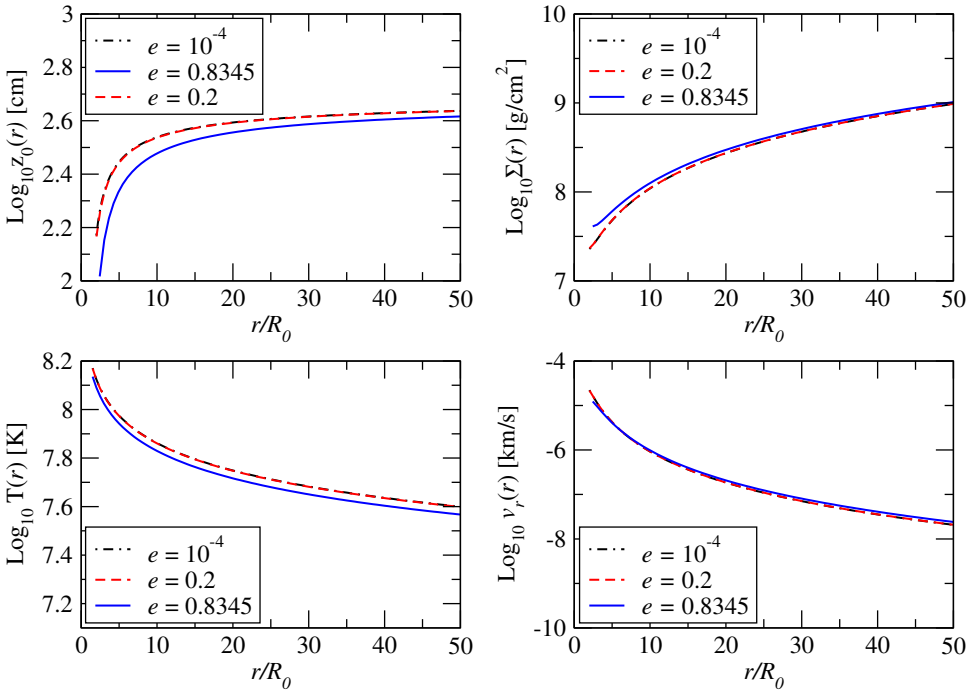

Figure 2. Multiplot shows radial variation of height $z_0(r)$, surface density $\Sigma(r)$, central temperature $T(r)$ and radial velocity $v_{\rm r}(r)$. The different chosen eccentricities are shown by $e = 10^{-4}$ (*black dotted-dashed curve*), $e = 0.2$ (*red dashed curve*) and $e = 0.8345$ (*solid blue curve*). This color convention for chosen eccentricities is same throughout the article. The right upper panel shows the logarithmic radial variation of the surface density $\Sigma(r)$. The left lower panel shows the logarithmic radial variation of the central temperature $T(r)$. The lower right panel shows the logarithmic radial variation of the radial velocity $v_{\rm r}(r)$ of the accreting matter.

3.2 Emitted Spectra from the disk

A very useful quantity for observational interest is emitted spectra from the accretion disk. Emitted spectra also corresponds to the size of accretion disk. We computed spectra using surface temperature of the disk. We chose a fixed outer radius of the accretion disk to see the behaviour of the emitted spectra with change in eccentricity. The accretion disk we assumed here is optically thick in the z direction therefore we can assume that each element of the disk emits as black body with surface temperature $T_{\rm s}(r)$. Using angular velocity from Eq. (2) and equating the dissipation rate per unit area to the black body flux we computed surface temperature $T_{\rm s}(r)$ of the accretion disk. Using the calculated temperature we can calculate intensity and with intensity emitted spectra of the accretion disk.

$$T_s(r) = \left[\frac{\dot{M} r \Omega T_1(r)}{4\pi\sigma}\frac{{\rm d}\Omega}{{\rm d}r}\right]^{1/4} \tag{26}$$

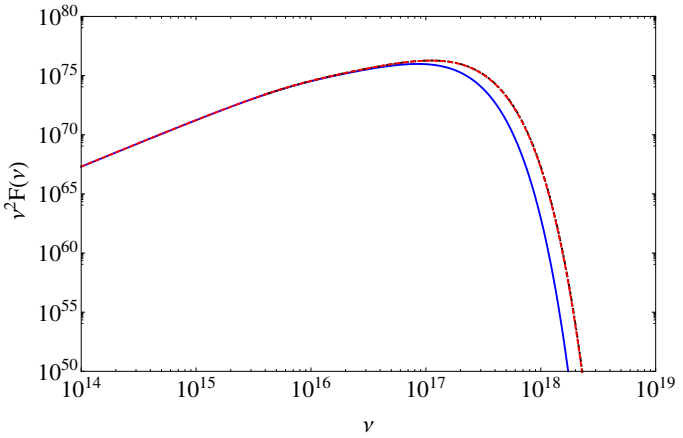

Figure 3. Logarithmic plot shows the emitted spectra from the accretion disk. *Black dotted dashed* curve corresponds to $e = 10^{-4}$, *red dashed* curve corresponds to $e = 0.2$ and *blue solid* curve correspond to $e = 0.8345$.

where $T_1(r)$ is defined as

$$T_1(r) = 1 - \frac{\Omega(a)a^2}{\Omega(r)r^2} \tag{27}$$

approximating the disk emitted spectra with black body we have

$$I(\nu) = B_\nu[T_s(r)] = \frac{2h\nu^3}{c^2\left(e^{h\nu/kT_s(r)} - 1\right)}, \tag{28}$$

using Eq. (27) we computed flux emitted from accretion disk by integration over the whole disk.

$$F(\nu) = 2\pi \int_{a(e)}^{R_{\text{out}}} I(\nu) r \, \mathrm{d}r \tag{29}$$

the integration of Eq. (29) gives emitted spectra from the disk. Figure 3 shows the logarithmic variation of emitted spectra from the accretion disk for eccentricities $e = 10^{-4}$ (black dashed curve) $e = 0.2$ (red dashed curve) and $e = 0.8345$ (solid blue curve). We found difference in emitted spectra at low frequencies. At high frequencies the difference is very small for changes in eccentricity of Maclaurin spheroid.

3.3 Evolution of surface density

We studied the non-stationary accretion disk using model described in Section 2.3. We assumed an initial Gaussian density distribution of matter at a radial distance of $r = 1.5\,a$ as the initial condition to solve the diffusion equation (Eq. 21). In all the results of non-stationary disk the time is in viscous time scale, $t_{\text{visc}} = a^2/\nu$, a being the semi-major axis

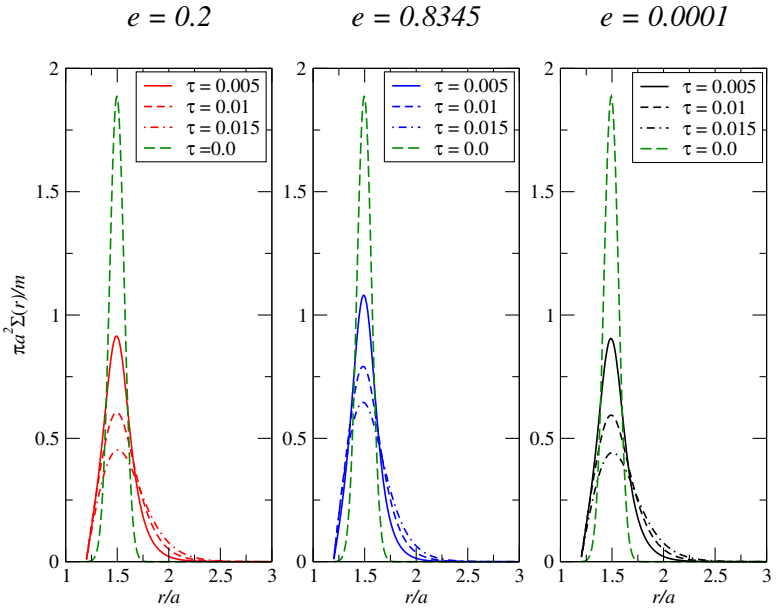

Figure 4. Time evolution of the ring of matter at a radial distance of $r = 1.5\,a$. The vertical axis shows the surface density scaled with initial surface density of ring of matter with mass m. The horizontal axis corresponds to radial distance form the center of star.

of the star. In our model we are interested for constant viscosity prescription therefore the kinematic viscosity coefficient $\nu = 0.01$ (in code units) is constant throughout our numerical computation. In Figure 4 we plotted the time evolution of surface density for the ring of matter at $r = 1.5\,a$ for $e = 10^{-4}$, $e = 0.2$ and $e = 0.8345$. The vertical axis shows the surface density $\Sigma(r)$ scaled with initial surface density. The horizontal axis corresponds to radial distance from the center of star scaled with semi-major axis a of the Maclaurin spheroid.

We also tested our numerical code by reducing the code parameters to the limiting case of spherically symmetric potential. In the appendix various code parameters are defined in which we chose parameter D (Eq. A2) which corresponds to the diffusion of matter. Figure 5 shows the variation of D with radial distance for eccentricities $e = 10^{-4}$ (black dotted-dashed curve), $e = 0.2$ (red dashed curve) and $e = 0.8345$ (solid blue curve). The limiting value in case of Keplerian angular velocity or $e = 0.0$ is $D = -3.0$. We see from Fig. 5 that as we decrease the eccentricity, parameter D is converging to $D = -3.0$. Also for larger radial distance the parameter D converges to the limit of spherically symmetric potential ($D = -3.0$).

4 DISCUSSION AND CONCLUSIONS

We conclude that our implementation of Maclaurin spheroid potential causes changes in the steady state disk parameters like half thickness of the disk. We also see that the change in eccentricity of the Maclaurin spheroid gives small change in central temperature of the

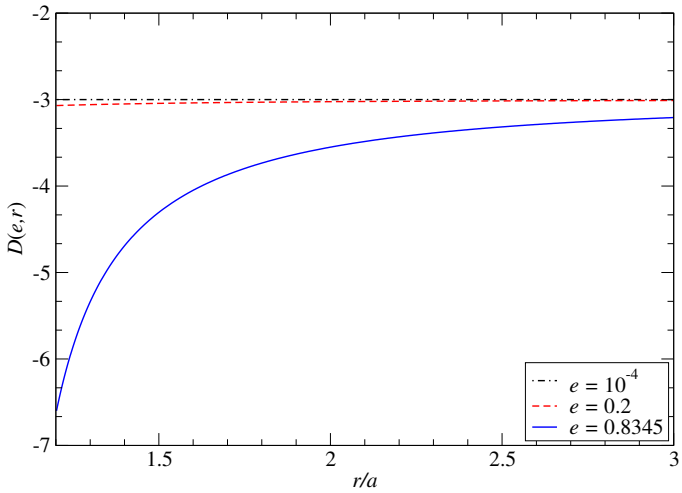

Figure 5. Plot shows the test of our code in the limiting case when $e \to 0$ (spherically symmetric object). The vertical axis shows the variation of the parameter D defined in Eq. (A2). The horizontal axis shows the radial distance form the center of star. Three different eccentricities $e = 10^{-4}$ (*black dotted-dashed curve*), $e = 0.2$ (*red dashed curve*) and upper limit in our model $e = 0.8345$ are plotted.

accretion disk. The radial velocity in case of steady state disk is inversely proportional to the corresponding surface density profile. This gives a very minor change in radial velocity profile for different eccentricities.

We computed the disk spectra for three values of eccentricity $e = 10^{-4}$, $e = 0.2$ and $e = 0.8345$. We know from the existing results that a change in the disk area changes the emitted spectra. In this paper the only parameter we changed is the eccentricity and a change in the eccentricity of the Maclaurin spheroid is changing the semi-major axis of the star as well as surface temperature $T_s(r)$. This small change in inner radius of the disk due to change in semi-major axis and change in surface temperature $T_s(r)$ causes a change in emitted spectra from the inner region of the accretion disk. The emitted spectra is affected only at high frequency region because this is emitted from inner parts of the accretion disk where Maclaurin spheroid potential dominates.

The results of non-stationary accretion disk are also dependent on eccentricity of Maclaurin spheroid. We found that if the eccentricity of the central object is lower the viscous evolution of the accretion disk will be more rapid as compare to high eccentricity. The choice of initial location of Gaussian distribution of matter is also important in our numerical model. We kept initial distribution of matter at $r = 1.5\,a$, which is very close to the Maclaurin spheroid. If we start at large radial distance as we can see from Fig. 5, the effect of eccentricity change will not be significant. From this result we can also explain that a spin-up or spin-down of the rapidly rotating Maclaurin spheroid can change the viscous evolution of the accretion disk. Maclaurin spheroid potential can also affect observed variability in the accretion disks around quark stars or white dwarfs. Change in viscous evolution and emitted spectra from disk can also observationally help in discriminating the neutron stars from quark stars, which is open astrophysics problem in scientific community.

ACKNOWLEDGEMENTS

We thank to Włodek Kluźniak for proposing this project. We also thank to F. H. Vincent and A. Manousakis for discussions. Research was supported by Polish NCN grant UMO-34 2011/01/B/ST9/05439 and 2013/08/A/ST9/00795.

REFERENCES

Amsterdamski, P., Bulik, T., Gondek-Rosińska, D. and Kluźniak, W. (2002), Marginally stable orbits around Maclaurin spheroids and low-mass quark stars, *Astronomy and Astrophysics*, **381**, pp. L21–L24, arXiv: `astro-ph/0012547`.

Birnstiel, T., Dullemond, C. P. and Brauer, F. (2010), Gas- and dust evolution in protoplanetary disks, *Astronomy and Astrophysics*, **513**, A79, arXiv: `1002.0335`.

Bisnovatyi-Kogan, G. S. (1993), A self-consistent solution for an accretion disc structure around a rapidly rotating non-magnetized star, *Astronomy and Astrophysics*, **274**, p. 796.

Gondek-Rosińska, D., Kluźniak, W., Stergioulas, N. and Wiśniewicz, M. (2014), Epicyclic frequencies for rotating strange quark stars: Importance of stellar oblateness, *Phys. Rev. D*, **89**(10), 104001, arXiv: `1403.1129`.

Khanna, S., Strzelecka, Z., Mishra, B. and Kluźniak, W. (2014), Eigenmodes of trapped horizontal oscillations in accretion disks, in Z. Stuchlík, G. Török and T. Pecháček, editors, *Proceedings of RAGtime 14–16: Workshops on black holes and neutron stars, Opava, Prague, 18–22 September/15–18 July/11-19 October '12/'13/'14*, pp. 145–158, Silesian University in Opava, Opava, ISBN 978-80-7510-126-6, in this proceedings.

Kluźniak, W. and Rosińska, D. (2013), Orbital and epicyclic frequencies of Maclaurin spheroids, *Monthly Notices Roy. Astronom. Soc.*, **434**, pp. 2825–2829.

Kovács, Z., Cheng, K. S. and Harko, T. (2009), Thin accretion discs around neutron and quark stars, *Astronomy and Astrophysics*, **500**, pp. 621–631.

Lynden-Bell, D. and Pringle, J. E. (1974), The evolution of viscous discs and the origin of the nebular variables., *Monthly Notices Roy. Astronom. Soc.*, **168**, pp. 603–637.

Mishra, B. and Vaidya, B. (2015), A geometrically thin accretion disc around a Maclaurin spheroid, *Monthly Notices Roy. Astronom. Soc.*, **447**, pp. 1154–1163, arXiv: `1411.6054`.

Novikov, I. D. and Thorne, K. S. (1973), Astrophysics of black holes., in C. Dewitt and B. S. Dewitt, editors, *Black Holes (Les Astres Occlus)*, pp. 343–450.

Shakura, N. I. and Sunyaev, R. A. (1973), Black holes in binary systems. Observational appearance., *Astronomy and Astrophysics*, **24**, pp. 337–355.

APPENDIX A: NON-STATIONARY ACCRETION DISK

In this section we shall describe the different terms which we calculated for our model to fit with Eq. (A1)

$$\frac{\partial \Sigma}{\partial t} + \frac{\partial}{\partial r}(\Sigma u) - \frac{\partial}{\partial r}\left[hD\frac{\partial}{\partial r}\left(\nu\frac{\Sigma}{h}\right)\right] = L\Sigma\,, \tag{A1}$$

where

$$D = r\Omega'/\left(2\Omega + r\Omega'\right)\,, \tag{A2}$$

$$u = \nu\Omega'/\left(2\Omega + r\Omega'\right)\,, \tag{A3}$$

$$h = 1/r^3\Omega'\,, \tag{A4}$$

$$L = -\nu r^3\Omega'\left[\frac{3}{r^4 l_1} + \frac{3\Omega' + r\Omega''}{r^3 l_1^2}\right]\,, \tag{A5}$$

where again,

$$l_1 = \left(2\Omega + r\Omega'\right)\,. \tag{A6}$$